J Solid State Electrochem (2011) 15:1271–1277
DOI 10.1007/s10008-010-1201-y

ORIGINAL PAPER

The effects of polymer gel electrolyte composition on performance of quasi-solid-state dye-sensitized solar cells

Xiaodong Li · Dingwen Zhang · Xi Jiang Yin · Si Chen · Jianhua Shi · Zhuo Sun · Sumei Huang

Received: 15 July 2010 / Revised: 15 September 2010 / Accepted: 17 September 2010 / Published online: 29 September 2010

Abstract Polymer gel electrolytes based on poly(acrylic acid)-poly(ethylene glycol) (PAA–PEG) hybrid have been prepared and applied to developed quasi-solid-state dye-sensitized solar cells (DSCs). PAA–PEG hybrid was synthesized by polymerization reaction. Quasi-solid-state DSCs were fabricated with synthesized PAA–PEG electrolyte. The effects of alkali iodides LiI, KI, and I_2 concentrations on liquid electrolyte absorbency and ionic conductivity of PAA–PEG were investigated. The evolution of the solar cell parameters with polymer gel electrolyte compositions was revealed. DSCs based on PAA–PEG with optimized KI/I_2 concentrations showed better performances than those with optimized LiI/I_2 concentrations. The electrochemical impedance spectroscopy technique was employed to examine the electron lifetime in the TiO_2 electrode and quantify charge transfer resistances at the TiO_2/dye/electrolyte interface and the counter electrode in the solar cells based on the PAA–PEG hybrid gels. A maximum conversion efficiency of 4.96% was obtained for DSCs using KI based quasi-solid electrolyte under 100 mW cm^{-2}. Our work suggests that KI can be the promising alkali metal iodide for improving the performance of PAA–PEG hybrid gel DSCs.

Keywords Quasi-solid-state · Dye-sensitized solar cells · Polymer gel electrolyte · Poly(acrylic acid)-poly(ethylene glycol)

X. Li · D. Zhang · S. Chen · J. Shi · Z. Sun · S. Huang (✉)
Engineering Research Center for Nanophotonics and Advanced Instrument, Ministry of Education, Department of Physics,
East China Normal University,
North Zhongshan Rd. 3663,
Shanghai 200062, People's Republic of China
e-mail: smhuang@phy.ecnu.edu.cn

X. Li · X. J. Yin
Advanced Materials Technology Centre, Office of the Chief Technology Officer, Singapore Polytechnic,
500 Dover Rd.,
Singapore, Singapore139651

Introduction

Since Grätzel's discovery of dye-sensitized solar cells (DSCs) in 1991 [1], the dominance of the photovoltaic field by inorganic solid-state junction devices has been challenged by the emergence of this third generation solar cells due to their low costs and steady efficiency. They offered an alternative conceptual approach rivaling conventional photovoltaic silicon and thin film solar cells. Many groups have focused their efforts on improving and comprehending different aspects of this technology. The liquid electrolyte usually employed in this cell is still a drawback for long-term practical operation due to electrolyte leakage or evaporation, and also makes large-scale production difficult. To overcome these problems, many research groups have been searching for alternatives to replace the liquid electrolytes with solid or quasi-solid-state hole-conductors, such as p-type semiconductors [2], organic hole conductors [3] and polymer gel electrolytes (PGEs) [4]. Among them, PGEs are considered as one kind of the most prospective substitutes for liquid electrolytes to fabricate practical quasi-solid state DSCs due to their merits such as easier assembly with different types of sealants, high ionic conductivity, good interfacial filling properties and relatively high long-term stability. Many gel polymer systems have been employed, such as poly(ethylene oxide) [5–7], poly(acrylonitrile) [8], poly(methyl methacrylate)

[9], Poly(vinylidene fluoride-*co*-hexafluoro propylene) [10, 11], and others. However, some PGEs mainly using physical interactions between polymer chains to solidify liquid electrolytes are thermo-reversible and unstable, which means a rigorous sealing procedure is still need for fabricating DSCs with long-term stability.

Recently, Wu et al. [12–14] reported a PGE based on poly (acrylic acid)–poly(ethylene glycol) (PAA–PEG) hybrid. This PGE is thermo-irreversible and stable due to the 3D network structure of the swollen hybrid. PAA–PEG hybrid is a kind of efficient absorbent, which can absorb large amount of liquid electrolyte, resulting in formation of the PGE with quite great ionic conductivity. Wu et al. firstly studied the effects of NaI/I_2 concentrations on the properties of this PAA–PEG hybrid gel, and developed a quasi-solid-state DSC with an efficiency of 3.19% [12]. Then, they further improved the performances of the DSC by the electric additive pyridine [13, 14]. Different types of cations will affect the properties of polymer gel electrolytes. In order to further develop this PGE technology, liquid electrolyte systems with various cations must be tested, and the electronic and ionic processes in this kind of quasi-solid-state DSCs must be explored and evaluated.

In this paper, PAA–PEG hybrid was synthesized by a polymerization reaction. The polymer gel electrolyte was fabricated by soaking the grown PAA–PEG in a conventional organic liquid electrolyte. The effects of the alkali metal iodides LiI, KI, and of I_2 concentrations on liquid electrolyte absorbency and ionic conductivity of the fabricated PGE as well as photovoltaic performance of the formed quasi-solid-state DSCs were investigated. The electrochemical impedance spectroscopy (EIS) technique was employed to explore and characterize electronic and ionic processes in the quasi-solid-state DSCs based on PAA–PEG hybrid gels.

Experimental

Synthesis of PAA–PEG hybrid and polymer gel electrolytes

PAA–PEG hybrid was synthesized according to the procedures reported in reference [12]. In brief, first, PEG (M_w=20,000) was dissolved in 5 ml distilled water. After being sufficiently stirred, the mixture was labeled as A. Next, 7.2 ml acrylic acid monomers and 0.1 wt% monomers of N, N′-methylene bisacrylamide were dissolved in 5 ml distilled water under stirring. Ammonium persulfate and sodium pyrosulfite (2 wt% of monomers) with an equivalent mole ratio were added as room temperature redox initiators to initiate the polymerization reaction. The resulted mixture was labeled as B. When the mixture B became a viscous solution, oligo-PAA was obtained. Then, mixture A was added into mixture B drop-by-drop while being sufficiently stirred to form a homogeneous hybrid. The polymerization reaction occurred when the hybrid was heated to 80 °C. The hybrid was kept in an ambient environment until the polymerization reaction was completed, and then moved into a vacuum oven at 80 °C to remove the water in the hybrid. Finally, the PGE was prepared by soaking hybrid obtained in a conventional liquid electrolyte.

Preparation of TiO_2 electrodes

Nanocrystalline films were prepared by employing commercial TiO_2 powder P25 (Degussa AG, Germany). The screen printed pastes were prepared according to the procedures mentioned in reference [15]. Under ambient conditions, the P25 nanoparticles were ground in an agate mortar. Acetic acid (1 ml), distilled water (5 ml), and ethanol (30 ml) were added gradually drop-by-drop to disperse the nanoparticles which were continuously ground. The TiO_2 dispersions were transferred with ethanol (80 ml) to a tall beaker, and stirred with a large magnetic bar at 300 rpm. Anhydrous terpineol and a mixture solution of ethyl celluloses in ethanol were added, followed by stirring and sonication. A Ti-horn-equipped sonicator (Sonifier 250, Branson Ultrasonics Corporation, Danbury, CT, USA) was used to perform the ultrasonic homogenization. The TiO_2 dispersions were concentrated by evaporating ethanol with a rotary evaporator. The TiO_2 pastes were finalized by grinding in the mortar one further time.

The flurorine-doped SnO_2 transparent conducting oxide (FTO) glass was first cleaned in detergent, then washed with distilled water and treated with 40 mM $TiCl_4$ aqueous solution at 70 °C for 30 min. A TiO_2 layer with a thickness of 12~14 μm was deposited on the pre-treated conducting glass using the formed TiO_2 paste using the screen printing technique. The thickness of films was determined by a surface profiler (Dektak 6 M, Vecco, USA). The screen-printed layer was gradually heated in air at 450 °C for 15 min and 500 °C for 15 min, to remove all organic components and to establish sufficient interconnects between nanoparticles. Finally, the formed TiO_2 electrodes were treated with 40 mM $TiCl_4$ solution, washed with distilled water and ethanol, and sintered again at 500 °C for 30 min in air.

Fabrication of quasi-solid-state dye-sensitized solar cells

After the second heat treatment at 500 °C and cooling to 80 °C, the TiO_2 electrodes were dye-coated by immersing into a solution of 0.5 mM dye N719 (Solaronix SA Co., Switzerland) in acetonitrile and tert-butyl alcohol (volume ratio of 1:1) at room temperature for 20–24 h, and then

assembled with thermally platinized conducting glass electrodes into DSC cells by sandwiching a slice of the fabricated PGE. The cells were sealed with 25 μm thick Surlyn 1702 (Dupont) gaskets. The cell size is 0.196 cm^2.

Measurements

The morphology of the polymer hybrid was characterized by field emission-scanning electron microscope (FESEM; JSM-7001F JEOL, Japan). The liquid electrolyte absorbency (Q) of hybrid was defined as:

$$Q = \frac{W - W_0}{W_0} \times 100\% \quad (1)$$

Here, W is the weight of swollen hybrid, and W_0 is the original weight of dry hybrid. The Q values of samples were calculated according to Eq. 1. Ion conductivity was measured using a multi-parameter tester (model PCSTestr 35, Eutech Instruments, Singapore).

Photocurrent–voltage (I–V) measurements were performed using an AM 1.5 solar simulator (model Oriel 91192, Irvine CA, Newport, USA). The solar simulator was calibrated by using a standard Silicon cell (model 91150 V, Irvine CA, Newport, USA). The light intensity was 100 mW cm^{-2} on the surface of the test cell. I–V curves were measured using a computer-controlled IV tracer (model VS-6810, Industrial Vision Technology (S) Pte Ltd, Singapore). During the I–V measurement, a mask with an aperture slightly bigger than the active area of the measured cell was used. It is very important to use a standard AM 1.5 solar simulator and apply a suitable mask covering the solar cell to do the I–V measurements. Otherwise, the efficiency of the measured cell will be overestimated for up to 30% [16].

EIS measurements of the DSCs were recorded with a potentiostat/galvanostat (PG30.FRA2, Autolab, Eco Chemie B. V Utrecht, The Netherlands) under illumination of 100 mW cm^{-2}. The frequency range was from 0.01 Hz to 100 kHz. The applied bias and ac amplitude were set at open-circuit voltage of the DSCs and 10 mV between the Pt counter electrode and the TiO_2 working electrode, respectively. The obtained spectra were fitted with Z-View software (V3.10) in terms of appropriate equivalent circuits.

Results and discussion

Figure 1 shows a typical digital photograph of the PAA–PEG hybrid before and after soaking in liquid electrolyte. As shown in the Fig. 1b, the uniform deep color of the hybrid after an uptake of liquid electrolyte indicated that the hybrid had fully absorbed liquid electrolyte. Moreover, the absorbed liquid electrolyte was not released from the hybrid even under pressure. The morphology of the top surface of the swollen hybrid is shown in Fig. 2a and b. In Fig. 2b (higher magnification), network structures and micro-sized (1–2 μm) microporous pores are clearly shown. The feature suggested the excellent swelling ability of the PAA–PEG hybrid in liquid electrolyte.

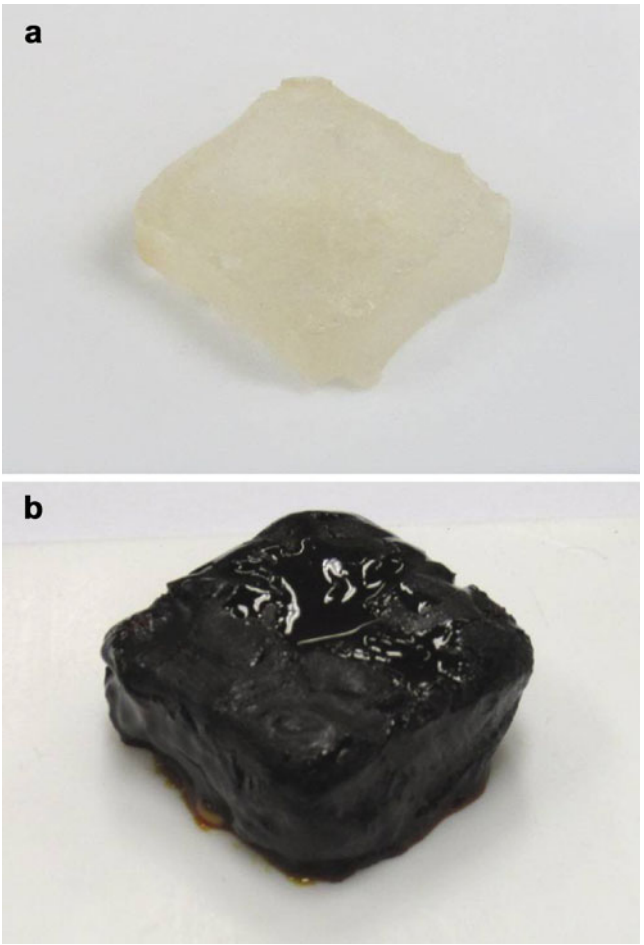

Fig. 1 Digital photograph of PAA–PEG before (**a**) and after (**b**) being soaked in liquid electrolyte

Figure 3 shows the dependence of liquid electrolyte absorbency and ionic conductivity of the formed PGE on different concentrations of LiI and KI. The liquid electrolyte used consisted of 0.05 M I_2 and 0.0–0.9 M LiI or KI in a mixed organic solvent of 30 vol%N-methylpyrrolidone (NMP) and 70 vol% γ-butyrolactone (GBL). Alkali metal iodides LiI and KI showed higher solubility than that of NaI in the mixed solvent. From Fig. 3, both iodide salts had a quite similar influence on the liquid electrolyte absorbency and ionic conductivity of the PGE produced. The liquid electrolyte absorbency increased when the concentration of LiI or KI increased from 0.0 to 0.1 M, achieving a maximal value at 0.1 M LiI or KI. When the LiI or KI concentration exceeded 0.1 M, the liquid electrolyte absorbency decreased with increasing

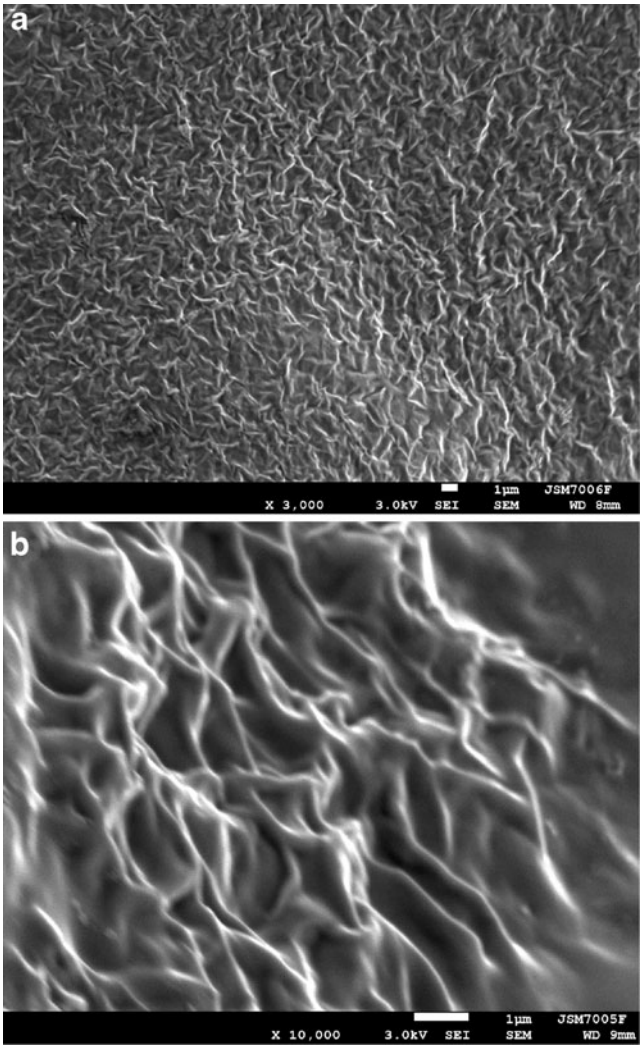

Fig. 2 SEM image of the formed polymer gel electrolyte (PGE)

the iodide concentration. On the other hand, the ionic conductivity of PGE increased when the concentration of LiI or KI increased from 0.0 to 0.5 M, reached a maximal value at 0.5 M LiI or KI, and then decreased when the concentration of iodide salt was further increased.

According to the adsorption mechanism of the PAA–PEG hybrid, the used mixed solvents penetrated into PAA–PEG hybrid by breaking parts of hydrogen bonds in the hybrid. Complexation interaction between cations (Li^+, K^+) and carbonyl or ether groups occurred in the hybrid when small amounts of alkali metal iodides were added into Lewis basic mixed solvents [12, 17], which destroyed hydrogen bonds and increased the liquid electrolyte absorbency. However, further increasing iodide concentration in liquid electrolyte led to the formation of large amount of linkages in PGE, which caused the shrinkage of PGE and the decrease of liquid electrolyte absorbency. In addition, with higher iodide (LiI, KI) concentration, the viscosity of the liquid electrolyte increased. The increase of the viscosity hindered penetration of liquid electrolyte into the PAA–PEG hybrid. As a result, the liquid electrolyte absorbency of the hybrid decreased when the iodide concentration was further increased from 0.1 M. From Fig. 3, the liquid electrolyte absorbency of PGE reached a maximal value at 0.1 M LiI or KI, however, the values attained were different. Cations affected the interfacial energetics of polymer gel electrolyte. As the radius of K^+ is larger than that of Li^+, K^+ led to less complexation interaction between positive ions and carbonyl or ether groups in the hybrid and less linkages in PGE, and resulted in a small increase in the maximal value of liquid electrolyte absorbency as shown in Fig. 3.

The initial increase of the ionic conductivity with the concentration of iodide in Fig. 3 can be attributed to increasing of the liquid electrolyte absorbency and rising of Li^+ or K^+ and I^- concentrations. The increase of the liquid electrolyte absorbency resulted in the formation of highly and sufficiently swollen hybrid network and continuous organic solvent phase in PGE, which decreased the resistance of PAA–PEG hybrid matrix on ions transport. However, when the concentration of the iodide salt exceeded 0.5 M, the value of liquid electrolyte absorbency fell considerably and the resistance of PAA–PEG hybrid matrix to ion transport clearly increased, resulting in the decrease of the ionic conductivity. Compared to the case of KI, the slightly smaller maximal value of ionic conductivity of the PGE based on LiI can be associated with its slightly smaller liquid electrolyte absorbency value at 0.5 M LiI. The optimized concentration of LiI or KI is 0.5 M.

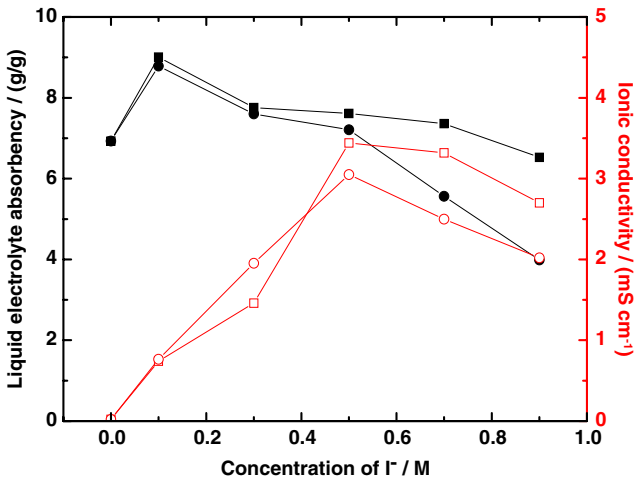

Fig. 3 Dependence of liquid electrolyte absorbency and ionic conductivity of PGE on concentrations of alkali metal iodides (LiI and KI; *filled square* liquid electrolyte absorbency of PGE containing KI, *filled circle* liquid electrolyte absorbency of PGE containing LiI, *open square* ionic conductivity of PGE containing KI, *open circle* ionic conductivity of PGE containing LiI). Electrolyte compositions: 0–0.9 M LiI or KI, 0.05 M I_2 in 30 vol% NMP and 70 vol% GBL mixed solvents

It was found that the concentration of I_2 in the liquid electrolyte also exerted a great influence on the physical properties of the PGE. Liquid electrolytes containing 0.5 M LiI or 0.5 M KI, 0.01–0.09 M I_2 in 30 vol% NMP and 70 vol% GBL mixed solvents were used for optimizing I_2 concentration. As shown in Fig. 4, for both LiI and KI electrolytes, the liquid electrolyte absorbency and the ionic conductivity of PGE increased in the low I_2 concentration range and then slowly decreased with increase of I_2 concentrations. The maximal liquid electrolyte absorbency occurred at I_2 concentrations of 0.03 and 0.01 M, while the maximum ionic conductivity occurred at I_2 concentrations of 0.07 and 0.05 M, for LiI and KI electrolytes, respectively.

I_2 additive supplies triiodide ions in PEG. The triiodide ions may block the complexation interaction between Li^+/K^+ and carbonyl or ether groups in hybrid because of their large volume, which breaks down some linkages in PGE formed by the complexation interaction. Fewer PGE linkages result in higher liquid electrolyte absorbency. In the case of electrolyte based on KI, the electrolyte absorbency increased until I_2 concentration reached 0.01 M. When the I_2 concentration was further increased from 0.01 M, the rising amount of triiodide resulted in the increase of the viscosity of the liquid electrolyte. The high viscosity was a disadvantage for the liquid electrolyte penetrating into the PAA–PEG hybrid. Thus, the liquid electrolyte absorbency decreased with the increase of I_2 concentration from 0.01 to 0.09 M as shown in Fig. 4. However, in the electrolyte based on LiI, due to the smaller radius of Li^+, more complexation interaction may occur in the PGE, and more triiodide ions may be needed to break down the complexation interaction. Therefore, the liquid electrolyte absorbency continuously increased with the I_2 concentration at low concentration range until I_2 concentration reached 0.03 M, and then decreased with I_2 concentration, as shown in Fig. 4. The maximum liquid electrolyte absorbency occurred at the higher I_2 concentration for LiI electrolyte system. This resulted in a maximum ionic conductivity at a higher I_2 concentration in PGE containing LiI compared with one containing KI. The maximum ionic conductivity values of 4.01 and 5.52 mS cm^{-1} were obtained for LiI and KI electrolytes, respectively. Therefore, the optimized I_2 concentration in electrolyte system containing 0.5 M LiI or 0.5 M KI was 0.07 and 0.05 M, respectively.

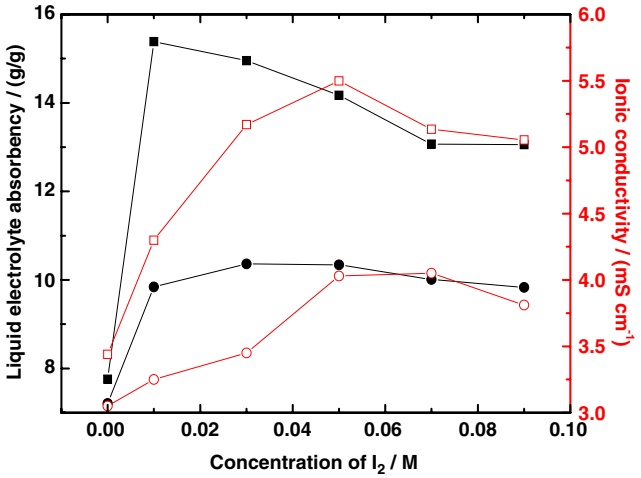

Fig. 4 Dependence of liquid electrolyte absorbency and ionic conductivity of PGE on I_2 concentration (*filled square* liquid electrolyte absorbency of PGE containing KI, *filled circle* liquid electrolyte absorbency of PGE containing LiI, *open square* ionic conductivity of PGE containing KI, *open circle* ionic conductivity of PGE containing LiI). Electrolyte compositions: 0.5 M LiI or KI, 0.01–0.09 M I_2 in 30 vol% NMP and 70 vol% GBL mixed solvents

Table 1 shows the dependence of the quasi-solid-state DSC photovoltaic performance on the I_2 concentration. The liquid electrolytes used contained 0.01–0.09 M I_2, 0.5 M LiI or 0.5 M KI in 70 vol% GBL and 30 vol% NMP mixed solvents. For both LiI and KI electrolytes, the open-circuit voltage (V_{oc}) was found to decrease somewhat with increasing I_2 concentration, while the cell efficiency (η) and the fill factor (FF) increased with I_2 concentration and then decreased when I_2 density was relatively high. An increase of the I_2 content led to an increasing concentration of I_3^-, inducing lower V_{oc} because of the enhanced parasitic electron back transfer reaction from TiO_2 conduction band electrons. It has been reported that V_{oc} at 82 mW cm^{-2} decreases by around 65 mV per tenfold increase in iodine concentration [18]. According to the Butler Volmer equation [19], low I_3^- concentrations resulted in lower currents at the counter electrode and consequently led to the lower DSC fill factors shown in Table 1. Another physical and chemical factor is that iodine absorbed violet and blue light and thus might significantly limit photocurrents with increasing concentration [20]. From Table 1, the best results were obtained at I_2 concentrations of 0.05 and 0.07 M for KI and LiI, respectively, as judged by the cell efficiency. Therefore, the evolution of the cell efficiency with the increase of I_2 concentration shown in Table 1 corresponds to the change of PGE ionic conductivity with increasing I_2 concentration shown in Fig. 4. Moreover, the DSC based on PGE with the optimized KI/I_2 concentrations showed higher η, FF, V_{oc} and short-circuit photocurrent density (J_{sc}) than those with optimized LiI/I_2 concentrations, as shown in Table 1.

EIS analysis was performed to further elucidate the photovoltaic findings in PAA–PEG hybrid gel DSCs. The electrolyte compositions used were 0.5 M LiI+0.07 M I_2 or 0.5 M KI+0.05 M I_2 in 30 vol% NMP and 70 vol% GBL mixed solvents. The corresponding quasi-solid-state DSCs are referred to as devices A and B, respectively, in the following. Figure 5a and b show the Nyquist and Bode plots of the electrochemical impedance spectra of devices A

Table 1 Dependence of the photovoltaic performance of quasi-solid-state DSCs on I_2 concentration

Electrolyte compositions: 0.5 M LiI or 0.5 M KI, 0.0–0.09 M I_2 in 30 vol% NMP and 70 vol% GBL mixed solvents

I_2 (M)	LiI				KI			
	J_{sc} (mA cm^{-2})	V_{oc} (V)	FF	η (%)	J_{sc} (mA cm^{-2})	V_{oc} (V)	FF	η (%)
0.01	14.486	0.626	0.307	2.78	13.660	0.637	0.352	3.06
0.03	14.683	0.614	0.354	3.19	13.691	0.622	0.433	3.69
0.05	14.362	0.614	0.452	3.99	14. 643	0.629	0.539	4.96
0.07	14.456	0.616	0.493	4.39	13.320	0.613	0.555	4.53
0.09	14.435	0.607	0.473	4.14	13.946	0.607	0.506	4.28

and B, respectively. In general, the EIS spectrum of the DSC shows three semicircles in the measured frequency from 0.1 Hz to 100 kHz. The ohmic series resistance (R_s) in the high-frequency region corresponds to the electrolyte and the FTO resistance, while the resistances R_{ct1}, R_{ct2} and R_{diff} relate to charge transfer processes occurring at the counter electrode in the high-frequency region, at the TiO_2/dye/electrolyte interface, and in Warburg diffusion within the electrolyte in the low frequency range, respectively [21–24]. Table 2 shows the values of electron transport resistances R_{ct1}, R_{ct2}, and R_{diff} obtained by fitting the EIS spectra with the equivalent circuit shown in Fig. 5a. The values of transfer resistances R_{ct1} and R_{ct2} in devices A and B were very different.

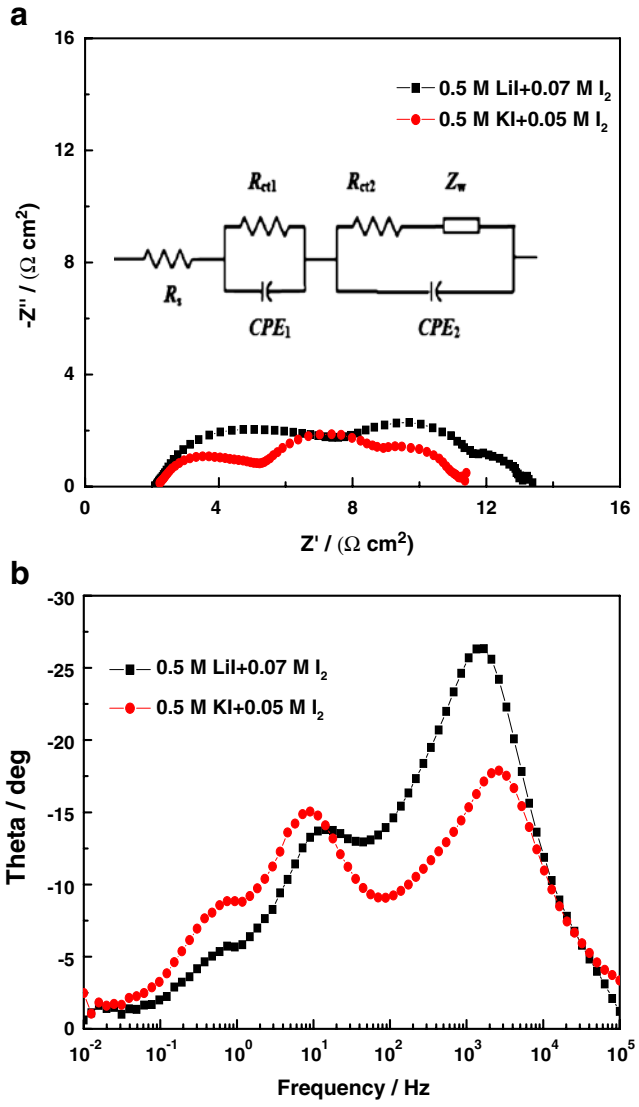

Fig. 5 Electrochemical impedance spectra of DSCs based on PGEs with the optimized electrolyte compositions of 0.5 M LiI, 0.07 M I_2 or 0.5 M KI, 0.05 M I_2 in 30 vol% NMP and 70 vol% GBL mixed solvents. **a** Nyquist plots, **b** Bode phase plots

From the Bode plots in diagrams in Fig. 5b, the middle-frequency peak (corresponding to the TiO_2/dye/electrolyte interface) of device B shifted to lower frequency relative to device A, indicating a longer electron lifetime in the TiO_2 electrode for the former. This result is in line with the corresponding photovoltaic performance values in Table 1. The increase of electron lifetime explained the higher V_{oc} observed in device B, since this parameter is strongly affected by the balance between the electron injection in TiO_2 and the recombination with I_3^- in the electrolyte [18, 21, 22]. From Fig. 5a and Table 2, device B showed lower transfer resistance R_{ct2} than device A. The lower R_{ct2} in device B suggested more redox couples penetrating into the pores of the TiO_2 electrode and more facile transport of the redox couple in the TiO_2 interface, thereby increasing J_{sc} and improving the cell efficiency shown in Table 1. On the other hand, the low- and high-frequency peaks observed in the Bode plots correspond to triiodide diffusion in the electrolyte and charge transfer at the counter electrode, respectively. In comparison with device A, the characteristic peak in the high-frequency regime (1 K∼100 kHz) in device B shifted to higher frequency shown in Fig. 5b,

Table 2 Electron transport resistances of DSCs based on PGEs with the optimized electrolyte compositions of 0.5 M LiI, 0.07 M I_2 or 0.5 M KI, 0.05 M I_2 in 30 vol% NMP and 70 vol% GBL mixed solvents

Optimized electrolyte	R_{ct1} (Ω cm^2)	R_{ct2} (Ω cm^2)	R_{diff} (Ω cm^2)
0.5 M LiI, 0.07 M I_2	5.78	9.54	5.02
0.5 M KI, 0.05 M I_2	3.56	5.71	4.99

meaning lower electron lifetimes and shorter redox reaction times at the platinum counter electrode and suggesting more redox reaction of I^-/I_3^- and the lower redox charge transfer resistance R_{ct1} at the counter electrode shown in Table 2. The lower R_{ct1} at the counter electrode in device B explained the smaller semicircle at left hand side of the Nyquist diagram (Fig. 5a). This situation is also consistent with higher FF in device B shown in Table 1. The result may be attributed to the activation or better contact between the electrolyte and the platinum catalyst. Finally, slightly lower diffusion resistance (R_{diff}) of I^-/I_3^- was observed for device B. Decreasing R_{diff} meant increasing ion mobility, hence improving the cell efficiencies in device B. As a result, the DSC based on PGE with the optimized KI and I_2 concentrations showed higher efficiency than that with the optimized LiI and I_2 concentrations shown in Table 1.

From Table 1, the maximum conversion efficiency of 4.96% was obtained with electrolyte contained 0.5 M KI, 0.05 M I_2, 70 vol% GBL and 30 vol% NMP under 100 mW cm^{-2} (AM 1.5) irradiation using a standard AM 1.5 solar simulator and a mask with an aperture slightly larger than the cell active area. This value is higher than those of PAA–PEG hybrid gel DSCs reported in refs [12, 13]. In these references, efficiencies of 3.19% and 4.74% under 100 mW cm^{-2} irradiation from a 100 W Xe arc lamp were reported for electrolytes composed of 0.5 M NaI, 0.05 M I_2, 0.5 M 4-tert-butylpyridine in GBL and 0.5 M NaI, 0.05 M I_2, 0.4 M pyridine, 70 vol% GBL and 30 vol% NMP, respectively. Nitrogen-containing heterocyclic additives such as 4-tert-butylpyridine and pyridine are thought to have ability to efficiently enhance the open-circuit photovoltage, fill factor, and the solar energy conversion efficiency [25]. Without using pyridine or 4-tert-butylpyridine, the better performance of our optimized cells can be attributed to the higher solubility of KI in 30 vol% NMP and 70 vol% GBL mixed solvent., which resulted in the formation of PGE with a high value of liquid electrolyte absorbency about 14.14 and a great value of ionic conductivity about 5.52 mS cm^{-1}, thus improving the performance of solar cells.

Conclusions

A series of PGEs based on PAA–PEG hybrid were prepared and employed to fabricate quasi-solid-state DSCs. The effects of Li^+, K^+ and I_2 concentration on the liquid electrolyte absorbency and ionic conductivity of the PGE were studied. The photoelectrochemical behaviors of the quasi-solid-state DSCs were investigated under influences of different cations and I_2 concentrations. DSCs based on PGEs with the optimized KI/I_2 concentrations showed better performances than those with optimized LiI/I_2 concentrations. These observations were in line with the results obtained by electrochemical impedance spectroscopy. DSCs using KI-based quasi-solid-electrolyte achieved a maximum conversion efficiency of 4.96% under 100 mW cm^{-2} (AM 1.5) irradiation.

Acknowledgments This work was supported by National Natural Science Foundation of China (No. 10774046), Shanghai Municipal Science and Technology Committee (No.09JC1404600, No.0852 nm06100 and No.08230705400) and Singapore Ministry of Education innovation fund (MOE IF Funding MOE2008-IF-1-016).

References

1. O'Regan B, Grätzel M (1991) Nature 353:737–740
2. Tennakone K, Perera V, Kottegoda I, Kumara G (1999) J Phys D Appl Phys 32:374–379
3. Bach U, Lupo D, Comte P, Moser JE (1998) Nature 395:583–585
4. Wang P, Zakeeruddin SM, Moser JE, Nazeeruddin MK, Sekiguchi T, Grätzel M (2003) Nat Mater 2:402–407
5. Stergiopoulos T, Arabatzis IM, Katsaros G, Falaras P (2002) Nano Lett 2:1259–1261
6. Katsaros G, Stergiopoulos T, Arabatzis IM, Papadokostaki KG, Falaras P (2002) J Photochem Photobiol A 149:191–198
7. Kim YJ, Kim JH, Kang MS, Lee MJ, Won J, Lee JC, Kang YS (2004) Adv Mater 16:1753–1757
8. Cao F, Oskam G, Searson PC (1995) J Phys Chem 99:17071–17080
9. Yang H, Huang ML, Wu JH, Lan Z, Hao SC, Lin JM (2008) Mater Chem Phys 110:38–42
10. Zhang J, Han HW, Wu SJ, Xu S, Zhou CH, Yang Y, Zhao XZ (2007) Nanotechnology 18:295606
11. Zhang DW, Li XD, Sun Z, Chen YW, Huang SM (2008) The 2nd IEEE International Nanoelectronics Conference (INEC 2008):1335–1339
12. Lan Z, Wu JH, Lin JM, Huang ML (2007) J Power Sources 164:921–925
13. Lan Z, Wu JH, Lin JM, Huang ML, Li PJ, Li QH (2008) Electrochim Acta 53:2296–2301
14. Wu JH, Lan Z, Lin JM, Huang ML, Hao SC, Sato T, Yin S (2007) Adv Mater 19:4006–4011
15. Ito S, Chen P, Comte P (2007) Prog Photovolt 15:603–612
16. Ito S, Nazeeruddin M, Liska P, Comte P (2006) Prog Photovolt 14:589–601
17. Kim JH, Kang MS, Kim YJ, Won J, Kang YS (2005) Solid State Ionics 176:579–584
18. Liu Y, Hagfeldt A, Xiao XR, Lindquist SE (1998) Sol Energy Mater Sol Cells 55:267–281
19. Peter LM (2007) Phy Chem Chem Phys 9:2630–2642
20. Hara K, Horiguchi T, Kinoshita T, Sayama K, Arakawa H (2001) Sol Energy Mater Sol Cells 70:151–161
21. Kern R, Sastrawan R, Ferber J, Stangl R, Luther J (2002) Electrochim Acta 47:4213–4225
22. Wang Q, Moser JE, Grätzel M (2005) J Phys Chem B 109:14945–14953
23. Han L, Koide N, Chiba Y, Islam A, Komiya R, Fuke N, Fukui A, Yamanaka RR (2005) Appl Phys Lett 86:213501–213504
24. Zhang DW, Li XD, Chen S, Tao F, Sun Z, Yin XJ, Huang SM (2009) J Solid State Electrochem. doi:10.1007/s10008-009-0982-3
25. Kusama H, Kurashige M, Arakawa H (2005) J Photochem Photobiol A: Chem 169:169–176